

A BOOSTER FREE FROM SPIN RESONANCES FOR FUTURE 100 KM-SCALE CIRCULAR e^+e^- COLLIDERS*

T. Chen¹, Z. Duan[†], D. H. Ji, D. Wang

Institute of High Energy Physics, Chinese Academy of Sciences, Beijing 10049, China

¹also at University of Chinese Academy of Sciences, Beijing 10049, China

Abstract

This paper reports the recent progress in the acceleration of polarized electron (positron) beams in a 100 km-scale booster lattice of the Circular Electron Positron Collider (CEPC). We have studied the structure of spin depolarization resonances of the lattice. The lattice features a high periodicity and analysis shows the contributions to the strengths of intrinsic and imperfection spin resonances add up coherently near the super-strong resonances beyond 120 GeV, but mostly cancel out and result in generally weak resonance strengths at lower beam energies. Detailed simulations confirm that beam polarization can be mostly maintained in the fast acceleration to 45.6 GeV and 80 GeV, but that severe depolarization may occur at even higher energies.

INTRODUCTION

The Circular Electron Positron Collider (CEPC) [1] is one of the future e^+e^- collider projects that aim to study the properties of the Higgs boson. Beam polarization is an important design aspect for CEPC. Longitudinally polarized colliding beams could provide an extra probe into the precision tests of the standard model as well as the search for new physics via colliding beam experiments. In order to achieve high polarization without significant sacrificing luminosity, polarized beams are generated from the source and injected into the collider rings. As the electron (positron) beam accelerates in a booster synchrotron, crossing of spin resonances could lead to beam depolarization. The polarization loss during the crossing of a single, isolated spin resonance can be estimated with the Froissart-Stora formula [2]

$$\frac{P_f}{P_i} \approx 2 \exp\left(-\frac{\pi |\tilde{\omega}_K|^2}{2\alpha}\right) - 1 \quad (1)$$

where P_i and P_f are the polarizations before and after the resonance crossing, and $\tilde{\omega}_K$ is the spin resonance strength, $\alpha = \frac{d\omega}{d\theta}$ is the spin resonance crossing rate. We can identify three parameter regimes in the value of $|\tilde{\omega}_K|/\sqrt{\alpha}$. Firstly, if the resonance is very strong, or when the acceleration is very slow, say $|\tilde{\omega}_K|/\sqrt{\alpha} > 1.84$, then $|\frac{P_f}{P_i}| > 99\%$ but with a change of sign relative to the initial value, i.e., a “spin flip”, and we call this the “slow crossing” regime. Second, if the resonance is very weak, or when the acceleration is very fast, say $|\tilde{\omega}_K|/\sqrt{\alpha} < 0.056$, then $|\frac{P_f}{P_i}| > 99\%$, and we

call this the “fast crossing” regime. Third, if both conditions are not satisfied, $|\frac{P_f}{P_i}|$ is reduced, and we call this the “intermediate” regime. There are two families of important spin resonances in this context: The integer spin resonances $\nu_0 = k$, mainly driven by the horizontal magnetic fields that arise from vertical orbit offsets, are also conventionally called the “imperfection resonances” [3]. The first-order “parent” spin resonances $\nu_0 = k \pm \nu_y$, driven by horizontal magnetic fields that arise from vertical betatron oscillations in quadrupoles, are also conventionally called the “intrinsic resonances” [3]. It is clear hundreds of spin resonances of these two families will be crossed in the acceleration .

In this work, we investigate the depolarization effects in the CEPC booster, by using a simplified lattice. Our analysis of the structure of spin resonances reveals similarities to previous research on the EIC booster [4], with relatively weak spin resonances within the range of working beam energies. Our estimates indicate that spin resonance crossings mostly occur within the “fast crossing” regime, resulting in minimal polarization loss during acceleration to 45.6 GeV and 80 GeV. However, at higher energies, such as during the acceleration to 120 GeV, depolarization is more significant. These analysis are verified by multi-particle tracking simulations. Our preliminary results were presented in [5], detailed results were presented in [6].

THE MODEL RING

The layout of a simplified model ring of the booster is shown in Fig. 1. The lattice is composed of 8 identical arc sections, 8 straight sections and 16 dispersion suppressor and matching (DOM) sections connecting them. The circumference of the booster is 100016.4 m, the same as the collider rings, of which 80% is the arc region. To reflect the

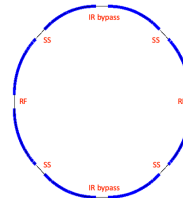


Figure 1: Layout of the candidate lattice for the CEPC booster.

influence of machine imperfections on beam polarization, we introduced misalignment errors and relative field errors of magnets, listed in Table 1, into the lattice. These errors were generated according to a Gaussian distribution trun-

* Work supported by National Key Program for S&T Research and Development (2018YFA0404300); National Natural Science Foundation of China (Grant No. 11975252 and 12275283); Youth Innovation Promotion Association CAS (No. 2021012)

† duanz@ihep.ac.cn

cated at $\pm 3\sigma$, we then performed closed-orbit correction and betatron-tune correction for these error seeds to restore the lattice performance. We scanned a range of rms BPM offset from 30 μm to 180 μm . For each setting of rms BPM offset, we accumulated 10 error seeds with converged closed-orbit correction and then obtain a collection of 60 error seeds for evaluation of the attainable polarization transmission.

Table 1: Magnet Error Settings

Component	Misalignment error				Field error
	Δx (μm)	Δy (μm)	Δz (μm)	$\Delta \theta_z$ (μrad)	
Dipole	100	100	100	100	0.05%
Quadrupole	100	100	100	100	0.02%
Sextupole	100	100	100	100	0.03%

INTRINSIC RESONANCES

To calculate the strengths of intrinsic resonances we used the DEPOL [3] code for the bare lattice and the sawtooth effect was not taken into account. As the strength of an intrinsic resonance depends on a particle's vertical betatron action I_y we calculated using a normalized vertical amplitude $\epsilon_{y,\text{norm}} = 2\gamma I_y$ of $10\pi\text{mm} \cdot \text{mrad}$. The resulting intrinsic-resonance spectrum is shown in Fig 2(a). It is clear that the first super-strong intrinsic resonance is above 120 GeV, below which the resonance strength generally increases with energy. For a Gaussian beam with an rms vertical emittance of $\epsilon_{y,\text{rms}}$, the depolarization when crossing a single intrinsic resonance at $\nu_0 = K$ is [7]

$$\frac{P_f}{P_i}(K, \epsilon_{y,\text{rms}}, \alpha) = \frac{1 - \frac{\pi |\tilde{\omega}_K^{\text{intr},\pm}(\epsilon_{y,\text{rms}})|^2}{\alpha}}{1 + \frac{\pi |\tilde{\omega}_K^{\text{intr},\pm}(\epsilon_{y,\text{rms}})|^2}{\alpha}} \quad (2)$$

Many intrinsic resonances would be crossed in the acceleration process. For an initial 100% vertically polarized beam, the vertical beam polarization at a certain time t during the acceleration $P_{\text{trans}}^{\text{intr}}(t)$ can be approximated by multiplying together the surviving polarization due to each intrinsic resonance the beam encounters before the time t . Then, the final polarization after the acceleration is $P_{\text{trans},f}^{\text{intr}} = P_{\text{trans}}^{\text{intr}}(t_{\text{ramp}})$. We chose a vertical equilibrium emittance of 100 pm at 120 GeV, and evaluated the evolution of the vertical rms emittance during the acceleration process. We scanned a range of vertical equilibrium emittance $\epsilon_{y,\text{eq},0}$ at a beam energy of 120 GeV. For each case, we used theoretical formula to evaluate the vertical rms emittance evolution during the acceleration. Then we estimate the polarization loss after crossing all intrinsic resonances in the acceleration process. The spin-resonance crossing rate was computed with real ramping curve. Results are showed in Fig 2(b). The depolarization caused by intrinsic resonances during acceleration to the Z and W energies is small. In contrast, the polarization loss in the H-mode depends strongly on $\epsilon_{y,\text{eq}}$.

IMPERFECTION RESONANCES

We implemented the algorithm of the DEPOL code in a Mathematica script using the closed orbit and optics func-

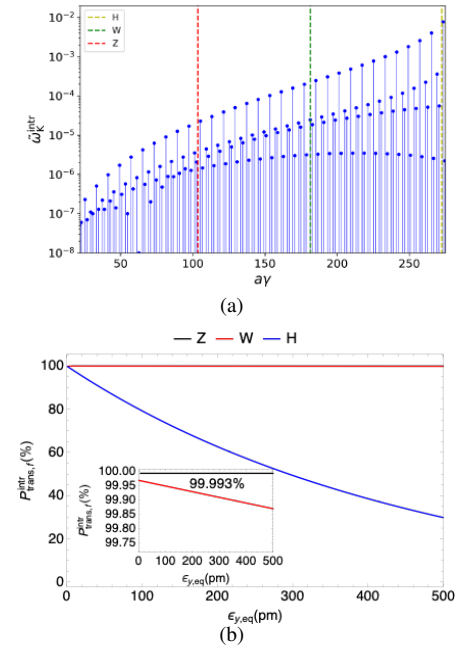


Figure 2: (a) shows the intrinsic-resonance spectrum in the working beam energy range. (b) shows the estimated final vertical polarization after crossing all the intrinsic resonances during the acceleration process. The inset plot shows a zoom-in view of the results of the Z-mode and the W-mode.

tions calculated by Bmad [8], where the sawtooth effect was not considered. The calculation took into account the major contributions due to quadrupoles, bends and sextupoles, as well as corrector fields inside the quadrupoles, but didn't consider the magnet roll errors nor the dipole relative field errors. Fig 3(a) illustrates the imperfection-resonance spectra for three error seeds with different vertical rms CODs in the working energy range. The strength of imperfection resonances generally increases with energy, with 120 GeV just below the first strong imperfection resonance. Besides, it is clear there is an increase in the strength of the strongest imperfection resonances just below 120 GeV for error seed 060 with the largest vertical rms COD.

We quantify the depolarization due to the crossings of imperfection resonances, using a method similar to that for intrinsic resonances. For an initial 100% vertical polarization, we can estimate the vertical polarization at a specified time t during acceleration, $P_{\text{trans}}^{\text{imp}}(t)$, by multiplying together the surviving polarization due to each imperfection resonance that the beam encounters before the time t ,

$$P_{\text{trans}}^{\text{imp}}(t) \approx \prod_{K \leq G\gamma(t)} \left[2 \exp\left(-\frac{\pi |\tilde{\omega}_K^{\text{imp}}|^2}{2\alpha}\right) - 1 \right] \quad (3)$$

Then, the final vertical polarization after the acceleration is $P_{\text{trans},f}^{\text{imp}} = P_{\text{trans}}^{\text{imp}}(t_{\text{ramp}})$. This implicitly assumes there is no correlation in the depolarization due to successive crossings of adjacent imperfection resonances.

We calculated the strengths of imperfection resonances for all 60 error seeds, and estimated the depolarization due to the crossings of these imperfection resonances, for the three operation modes. The results, shown in Fig. 3(b), indicate that the polarization loss generally increases with the vertical rms COD. However, the polarization loss also varies among error seeds with similar vertical rms CODs, due to the difference in the spectra and maximum strengths of the imperfection resonances. For the Z-mode and the W-mode, the depolarization is less than 1% and 20%, respectively. In contrast, in the acceleration to 120 GeV, the depolarization is much more severe, ranging from about 50% to almost complete depolarization. This is due to the presence of many dangerous imperfection resonances near 120 GeV.

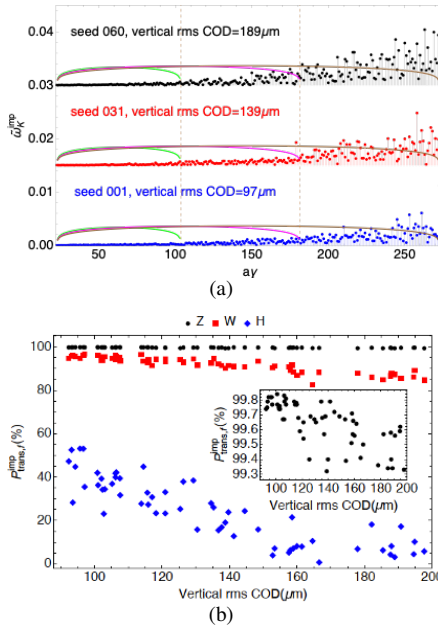


Figure 3: (a) shows the imperfection-resonance spectra of error seed 001, 031 and 060, an offset of 0.015 is appended to the latter two cases for comparison. The green, magenta and brown curves depict the upper strength limit for each imperfection resonance with the depolarization due to its crossing of less than 1%. (b) shows the estimated final vertical beam polarization after crossing all the imperfection resonances during the acceleration process. The inset plot shows a zoom-in view of the result for the Z-mode.

SIMULATION RESULTS

By combining these two contributions, we can now estimate the overall depolarization effects due to both types of resonances,

$$P_{\text{trans}}(t) \approx P_{\text{trans}}^{\text{intr}}(t) \times P_{\text{trans}}^{\text{imp}}(t) \quad (4)$$

and the final beam polarization after the acceleration is $P_{\text{trans},f} = P_{\text{trans}}(t_{\text{ramp}})$. We applied such estimation for all the 60 error seeds and referred to as the “estimation results”.

To verify our analysis, we utilized more realistic multi-particle tracking simulations of the acceleration process. For this we used the “long_term_tracking” option of BMAD and we tracked a Gaussian beam of 1000 particles with an initial vertical polarization of 100%. We set the ramping curves of the beam energy and the RF parameters, and turned on the radiation damping and quantum excitation effects in the element-by-element tracking with full six-dimensional orbit motion and three-dimensional spin motion. Hereafter we refer to the $P_{\text{trans},f}$ obtained using this method as the simulation results. The estimates and simulation results of $P_{\text{trans},f}$ for the 60 error seeds and the three operation modes are shown in Fig. 4.

These results suggest that a high-level of beam polarization can be maintained during the acceleration to 45.6 GeV and 80 GeV, but severe depolarization could occur at higher beam energies in the acceleration to 120 GeV. The key feature of the CEPC booster lattice is that all super-strong spin resonances are beyond the working beam energy range, though a few spin resonances near 120 GeV are still much enhanced. In fact, our test with several other candidate lattices of CEPC booster and collider rings confirmed that such a structure of spin resonances is a general feature of future 100 km-scale electron rings. This feature can be further exploited in the lattice design and optimization of these electron rings.

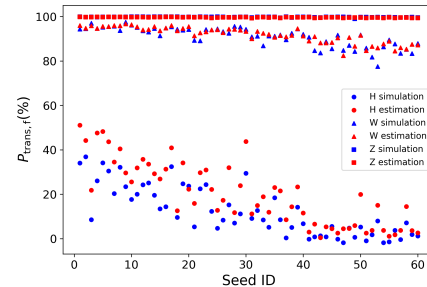


Figure 4: The final beam polarization after the acceleration $P_{\text{trans},f}$ for the 60 error seeds, assuming the injected beam is 100% vertically polarized.

CONCLUSION

The CEPC booster lattice has a high “effective” periodicity, making spacings between adjacent super-strong resonances large, while the first super-strong resonances also correspond to very high beam energies, within which the spin resonances are weak. Both analytical estimates and simulations confirmed the polarization losses during acceleration to 45.6 GeV and 80 GeV are tiny. However, the depolarization during acceleration to 120 GeV is more significant and further research is needed.

ACKNOWLEDGEMENTS

The authors are grateful to D. P. Barber and S. Nikitin for their helpful suggestions, to D. Sagan and E. Forest for kind help with Bmad/PTC.

REFERENCES

- [1] The CEPC Study Group, CEPC Conceptual Design Report Volume I-Accelerator , arXiv:1890.00285 (2018).
- [2] M. Froissart and R. Stora, Depolarisation d'un faisceau de protons polarisés dans un synchrotron, Nucl. Instrum. Methods. **7**, 297 (1960).
- [3] E. D. Courant and R. D. Ruth, The acceleration of polarized protons in circular accelerators, Tech. Rep. BNL 51270 (BNL, 1980).
- [4] V. H. Ranjbar, M. Blaskiewicz, F. Meot, C. Montag, S. Tepikian, S. Brooks, H. Witte, I. Marneris, V. Ptitsyn, and F. J. Willeke, Spin resonance free electron ring injector, Physical Review Accelerators and Beams 21, **111003** (2018).
- [5] Z. Duan et al., Longitudinally polarized colliding beams at the CEPC, Proc. eeFACT 2022, TUZAS0101 , 97 (2022).
- [6] T. Chen, Z. Duan, D. Ji, and D. Wang, “Spin Resonance Free Booster For Future 100 km-scale Circular e^+e^- Colliders,” arXiv:2302.05321 [physics], accepted by Phys. Rev. Accel. Beams, 2023.
- [7] S. Y. Lee, Spin dynamics and snakes in synchrotrons (World Scientific, 1997).
- [8] D. Sagan, The Bmad Reference Manual, <https://www.classe.cornell.edu/bmad/manual.html> (2023)